Available online at www.sciencedirect.com
SCIENCE DIRECT
Applied Clay Science 33 (2006) 13–20
Applied CLAY Science
www.elsevier.com/locate/clay

Preparation and performance of synthetic organoclays

J.C.A.A. Roelofs [a,*], P.H. Berben [b]

[a] Holland Colours N.V., Halvemaanweg 1 7323 RW, Apeldoorn, The Netherlands
[b] Engelhard de Meern B.V., Strijkviertel 67, De Meern, The Netherlands

Received 23 August 2005; received in revised form 27 February 2006; accepted 6 March 2006
Available online 2 May 2006

Abstract

A new type of organoclays was synthesized by a novel one-step-synthesis procedure using urea decomposition. The resulting organophilic material is a highly crystalline smectite with stevensite structure and dimethyl octadecylammonium cations in the interlayer and zinc cations within the layers. The stacking number of the layers is low, which facilitates exfoliation in olefinic polymers. Nanocomposites of low density polyethylene, without maleic anhydride modification, and 5% of the organoclay showed an increased thermal stability. The new organo-Zn-stevensite is capable of exfoliation, as observed with XRD and TEM, improving the properties of polymers without the need for maleic anhydride.

Keywords: Organoclays; Nanocomposites; Stevensite; Synthesis

1. Introduction

The field of nanocomposite science and technology has gained considerable interest over the last decade. Nanocomposites in the widest sense are defined as materials consisting of two or more components of which at least one dimension is in the nanometer range (Ajayan et al., 2003). Materials of interest are, amongst others, clay minerals with a layer thickness of 1 nm or lower. These (modified) clay minerals can be added to a wide variety of polymer, plastic and resin matrices to form inventive nanocomposite materials with improved structural strength. They can also be used for rheological purposes (Knudson et al., 1987), as flame retardant additives (Kausch et al., 2002) or in water purification applications (Cody and Kemnetz, 1997; Beall, 2003). Polymer nanocomposites have enhanced material properties, i.e. improved flame retardancy (Gilman et al., 2000), higher stiffness and toughness (Giannelis, 1996) and improved gas barrier properties (Yano et al., 1997). In general, the above-mentioned enhancements of properties are observed only at low clay loadings, typically 5 wt.% or less. At higher loading, the clay mineral platelets or agglomerates behave as normal fillers like glass and talc. The aspect ratio (i.e. lateral size of the particles divided by thickness) is considered as a key parameter to enhance material properties. Yano et al. (1997) showed that the longer the clay platelets were, the more effectively the properties of polyimide–clay hybrids were improved. Incomplete exfoliation of the particles, caused by the inability of the polymer to penetrate into thick stacks of layers, however, does not result in enhancement of properties, especially in the case of polymers more apolar than nylon-6. Key point is the dispersion of the clay particles in the matrix. Ideally,

* Corresponding author. Tel.: +31 55 3663143; fax: +31 55 3662981.
E-mail address: jroelofs@hollandcolours.com (J.C.A.A. Roelofs).

0169-1317/$ - see front matter © 2006 Elsevier B.V. All rights reserved.
doi:10.1016/j.clay.2006.03.001

during processing, the individual clay platelets will disperse uniformly into the polymer (exfoliation or delamination) giving the desired beneficial properties. In order to achieve compatibility of clay materials with apolar polymers, like polypropylene (PP) (Vaia and Giannelis, 1997a,b; Kawasumi et al., 1997; Reichert et al., 2000) and polyethylene (PE) (Wang et al., 2001), hydrated interlayer cations have been ion-exchanged by cationic surfactant onium ions such as alkylammonium or phosphonium salts (Maiti et al., 2002). Thus modified clays become organophilic and their surface energy is lowered. The ion-exchange procedure can go to completion or can be tailored to obtain heterostructures containing both organic and inorganic cations (Ijdo and Pinnavaia, 1999). The polymer itself is also often modified to increase compatibility and enhance interactions between organoclay and polymer, e.g. by using specials brands or combinations of maleic anhydride (MA)-grafted PE or PP (Mehta et al., 2003). Wang et al. (2001) prepared and characterized several maleated and non-maleated PE/clay nanocomposites. Melt-blended maleated PE with low MA levels of 0.1–0.2 and 5 wt.% of organoclay displayed a considerable exfoliation of the clay platelets. At lower MA levels and without MA intercalation of polymer into the clay interlayer was achieved as well. It was also stated that PE nanocomposites without MA could be obtained by proper modification of the clay only. Several reviews provide more information on these topics (Ogawa and Kuroda, 1997; Alexandre and Dubois, 2000; Manias et al., 2001; Vaia and Giannelis, 2001).

The synthesis of clay minerals according to the current state of the art is technically difficult. Generally, a prolonged hydrothermal treatment is performed at relatively high temperatures and pressures. In this respect, the industrial synthesis of hectorite is a good example. Together with montmorillonite (MMT), hectorite is the most applied material in the production of organoclays. In general, its industrial preparation starts from natural talc, which occurs amply in nature in pure form. After being crushed and mixed with lithium carbonate (Orlemann, 1972) or lithium/sodium hexafluorosilicate (Tateyama et al., 1993), this material is heated between 760 and 980 °C for approximately 1 h. In addition, sodium silicate and soda are added and the mixture is treated hydrothermally for 8–16 h. An example of MMT synthesis, which included a 72 h period hydrothermal treatment at 220 °C was published by Reinholdt et al. (2001). Other synthetic routes of hectorite have been described by Carrado et al. (1997, 2000). Interestingly, the use of synthetic smectites other than hectorite and MMT for the preparation of nanocomposites has not gained a lot of interest yet. However, it is known that saponite and stevensite can be synthesized under non-hydrothermal conditions, using the hydrolysis of urea to homogeneously increase the pH in order to precipitate the desired phase (Vogels, 1993; Vogels and Geus, 2001; Vogels et al., 2005). The structure of stevensite is represented by the formula $N^{z+}_{x/z}[M^{2+}{}_{6-x}\bullet)_x][Si_8]O_{20}(OH)_4{\cdot}nH_2O$ and it belongs to the class of trioctahedral smectites. Platelets are negatively charged, due to vacancies (•) in the cation layer. Application of this material is, up to now, limited to the use of heterogeneous support for hydrodesulfurization catalysts (Prihod'ko et al., 2002). In practice, stevensite is the most convenient smectite to synthesize, since the synthesis of saponite requires gel formation to preserve the tetrahedral coordination of Al. This process is difficult to scale up and almost always results in the presence of octahedrally coordinated Al in the smectite structure (Vogels, 1993; Kloprogge et al., 1999). In smectite clays, the nature of the octahedral cation markedly affects the dimensions of the resulting clay. The lateral platelet size of saponites increases with $Zn^{2+}>Co^{2+}>Ni^{2+}>Mg^{2+}$, whereas mixtures result in values between those of the respective homogeneous saponites (Vogels, 1993; Vogels and Geus, 2001). Zn^{2+} was our choice of metal cation, since the aspect ratio is considered to be of great importance for the final nanocomposite performance (Yano et al., 1997). However, several different undesired Zn-containing phases can (co-)precipitate when synthesis parameters (e.g. pH, temperature, Zn / Si ratio) are slightly altered. For instance, in a basic environment (pH 6–9) the synthesis of fraipontite $(Zn_{3-x}Al_x(Si_{2-x}Al_x)O_5(OH)_4$, a two-layer structure comprising a layer of tetrahedral silica and a ZnO_6 octahedral layer) can be performed (Usui et al., 1986; Kloprogge et al., 2001). The synthesis of sauconite, $Zn_3(Si,Al)_4O_{10},(OH)_2{\cdot}4H_2O$ can be switched to hemimorphite, $Zn_4Si_2O_7(OH)_2$, or willemite, Zn_2SiO_4, by increasing the temperature during hydrothermal treatment (Usui et al., 1987). More information on smectite synthesis can be found elsewhere (Kloprogge et al., 1999).

The current industrial production of organoclay materials involves various process steps, including purification of a natural clay in a diluted slurry, ion exchange of the (sodium) clay to incorporate a cationic organic compound and filtration (Bauer et al., 1993). One of the major problems associated with the use of natural clays is that, although these materials may be very cheap and readily available, the properties are very difficult to control due to fluctuation in purity and composition (Carrado, 2000). Examples of incomplete exfoliation of PP nanocomposites are known that were related to impurities (Kurokawa et al., 1996) or incomplete organophilization (Pozsgay et al., 2001).

Comparison of results obtained with differently or only partly purified organoclays hence becomes ambiguous.

We wish to report a new, direct synthesis route towards fully synthetic organoclays based on stevensite. Extensive characterization has been performed using XRD, TEM, TGA and elemental analysis. The obtained product is of high purity and crystallinity. Furthermore, the stacking of the layers is much less compared to other organoclays, which can facilitate the exfoliation process. First results obtained in low density polyethylene–organoclay nanocomposites preparation showed that their thermal stability is improved.

2. Experimental

2.1. Synthesis of organoclays

All chemicals were of p.a. quality, suitable for laboratory syntheses. A 3.3 l aqueous solution containing 300 g of 27 wt.% sodium silicate (Aldrich) with a initial pH of 1.5 (adjusted with concentrated nitric acid) was prepared. To this solution 300 g urea (Merck) and 300 g of $Zn(NO_3)_2{\cdot}6H_2O$ (Merck) was added and the dispersion was heated to 90 °C. When the temperature reached 65–70 °C, a hot solution of acidified dimethyloctadecylamine (Acros, 87%; 90–150 g in 1 l, around 25 ml of concentrated nitric acid was used to obtain a clear viscous solution) was added. The mixture was further heated to 90–100 °C and stirred for 16–20 h. After washing and drying a fluffy white powder was obtained, hydrophobic of nature and hereafter denoted as organo-Zn-stevensite. Yield was around 230–250 g.

Alternatively, the addition sequence of the components can be changed. For instance, when a solution containing the appropriate amounts of $Zn(NO_3)_2{\cdot}6H_2O$ and urea with a pH of 1.5 was poured into a solution containing sodium silicate and dimethyloctadecylamine (also having a pH of 1.5) at a temperature of 90 °C again the organo-Zn-stevensite was synthesized. The ICP analyses resulted in 18.8 wt.% Zn and 14.2 wt.% Si for $C_{18}C_2N$ (90) and 23.4 wt.% Zn and 15.8 wt.% Si in $C_{18}C_2N$ (150), where 90 and 150 represents the used amount of dimethyloctadecylamine.

2.2. Synthesis of Zn-stevensite

A Zn-stevensite sample was prepared according to the procedure of Vogels (1993). A solution containing the 300 g of $Zn(NO_3)_2{\cdot}6H_2O$, 300 g of 27 wt.% sodium silicate and 300 g urea with initial pH of 2–3 was heated to 90 °C and stirred for 24–48 h. After this, the white precipitate was washed and dried overnight at 110 °C.

The ICP analyses of the dried precipitate showed 26.3 wt.% Zn and 15.3 wt.% Si, resulting in a Zn / Si ratio = 0.74.

2.3. Nanocomposite formation

Low density polyethylene (LDPE, Hostalen GF 4760, DSM) with a Melt Flow Index (MFI) of 0.40 (190 °C/2.16 kg) was mixed with organo-Zn-stevensite powder (5 and 10 wt.%) and processed by melt-compounding at 130–140 °C using a Prism twin screw extruder with L / D = 24, 16 mm.

2.4. Characterization

Powder X-Ray Diffraction (XRD) patterns between 3.5° and 100° 2θ were obtained with a Philips PW 1710 diffractometer control (PW 1830 generator Cu-Kα radiation (40 kV, 45 mA). Slit size was 0.2 mm; scan step time 4.0 s). Low angle measurements (1.5–10° 2θ) were performed on a Philips PW 1820 apparatus. Transmission Electron Microscopy (TEM) images were obtained with a Philips CM-10. Ultrathin sections of the 5% organoclay in LDPE sample were prepared at room temperature using a diamond knife on a Reichert–Jung Ultramicrotomy apparatus. BET surface areas were obtained using a Micromeretics ASAP 2400. Prior to the measurements, samples were degassed at 80 °C under vacuum.

The standard protocol for the Inductively Coupled Plasma (ICP) analysis involved the following: A known amount of sample was mixed with a known amount of dilithium tetraborate and lithium bromide and placed in an oven and heated up to 1000 °C. The resulting pearl was dissolved in a nitric acid solution. The resulting solutions were measured using a Thermal Jarrell Ash Atom scan. The Thermal Gravimetric Analysis (TGA) and Differential Scanning Calorimetry (DSC) data were measured on a Rheometric Scientific PL-STA 1000 apparatus in air with a 10 °C/min heating rate.

3. Results and discussion

3.1. Organoclay synthesis and characterization

The role of urea is twofold: firstly, its decomposition results in a homogeneous release of hydroxyl ions, thus raising the pH and secondly it is vital in order to stabilize free Zn^{2+} in the solution. When sodium hydroxide was used to increase or maintain the pH at a constant level, a fast precipitation of $Zn(OH)_2$ (after drying of the precipitate present as ZnO) occurred at pH values exceeding 4.8, almost independent of temperature. When ammonia was present in a ratio of NH_3/ Zn = 4–5, $Zn(OH)_2$ precipitation was avoided due to the formation of the $Zn(NH_3)_4^{2+}$ complex. The stability of this complex also prevented the formation of the desired phase. When urea is used, it is likely that a complex similar to $Zn(NH_3)_4^{2+}$ is formed. The decomposition of urea probably results in a decreased stability of this Zn–urea complex, thus leading to a directed precipitation of Zn^{2+}. The initial pH was set at 1.5 and maintained at this value until all components had been added to the reaction vessel. A higher initial pH resulted in less favorable filtration properties and sometimes the (co-)formation of

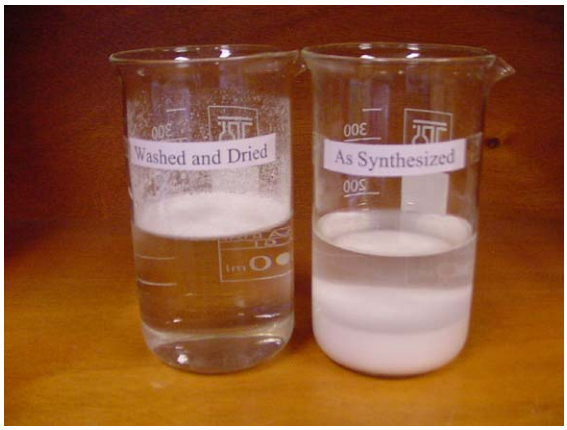

Fig. 1. Organo-Zn-stevensite synthesis dispersion after 24 h (right) Organo-Zn-stevensite powder (after washing and drying) showing the typical hydrophobic behaviour after exposure to water (left).

hemimorphite. After a synthesis time of 16–20 h, the white slurry contained the organoclay product which quickly settled after stirring was stopped. Only after washing and drying the organo-Zn-stevensite showed typically hydrophobic properties (Fig. 1). The BET surface areas of the dried organoclays were in the range of 50–80 m^2/g, comparable to the Zn-stevensite samples of Vogels (1993).

Fig. 2 shows the results of the XRD measurements. Besides the new organo-Zn-stevensite (Fig. 2B), the diffraction pattern of Zn-stevensite (Fig. 2A) is included. Both samples have the (060) reflection at a position of 1.54 Å (reflection at $2\Theta = 60°$), indicative of the trioctahedral smectite structure (Kloprogge et al., 1999). Several in-plane stevensite reflections did not change when the organo-Zn-stevensite was prepared, although changes of the reflections at 4.51 Å ($2\Theta = 19.2°$) and 3.2 Å ($2\Theta = 27.4°$) were observed. Likely, this is related to the composition of the interlayer space. The common basal spacing is around 13–15 Å in Zn-stevensite (Vogels, 1993; Kloprogge et al., 1999) (Fig. 2A). By subtracting the layer thickness of 1 nm, an interlayer space of around 4 Å for Zn^{2+} was calculated. The organo-Zn-stevensite has a much broader reflection at lower 2Θ values, due to the presence of protonated *N*, *N*-dimethyloctadecylamine. Broadening of the basal

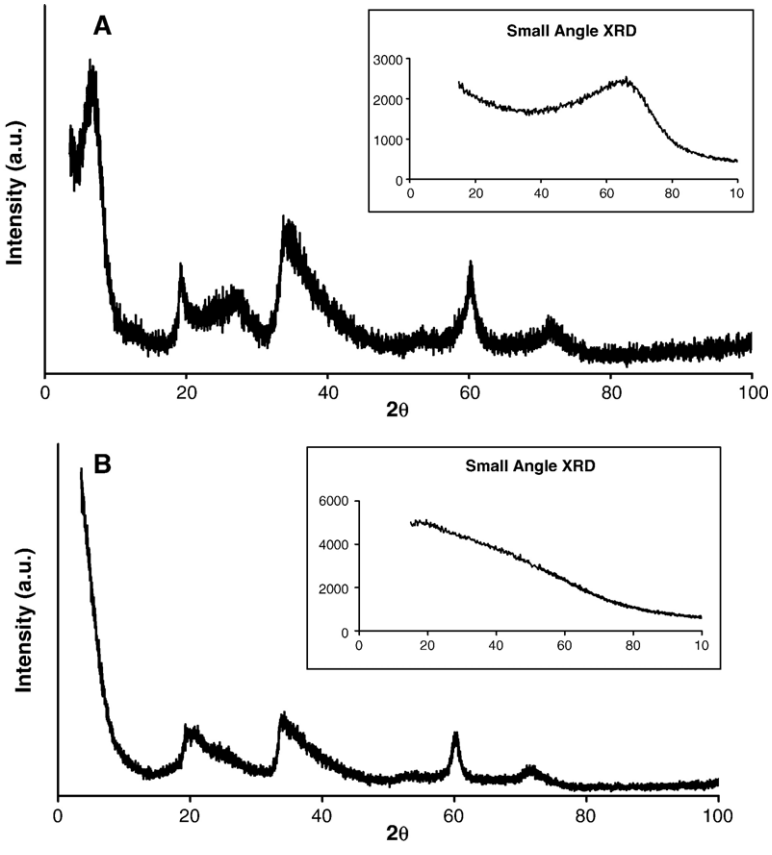

Fig. 2. XRD patterns of (A) Zn-stevensite (B) Organo-Zn-stevensite.

Table 1
Results of the organoclay syntheses from elemental analyses and calculations

Sample	Zn / Si	Reacted Si (%)	Reacted Zn (%)	C / N	N^+ / $\Delta Zn^{2+(1)}$	Corrected Zn / Si[(2)]	CEC[(3)] (meq/100 g)
$C_{18}C_2N$ (90)[(4)]	0.64	99	84	19	1.8	0.74	51
$C_{18}C_2N$ (150)[(4)]	0.57	100	79	19	2.1	0.72	32

[(1)]ΔZn^{2+} denotes the amount of unreacted Zn^{2+} (removed after washing).
[(2)]Molar amount calculated from elemental analysis: (Zn+2*N)/Si.
[(3)]Calculated using ΔZn^{2+} as charge compensating cation for the Cation Exchange Capacity ((elemental mass of Zn (g)/valence Zn^{2+})/1000 per 100 g of clay material).
[(4)]90 and 150 represent the used amount of $C_{18}C_2N$ in grams.

reflection is probably caused by a lack of long range order and low stacking number (vide infra).

Table 1 lists the elemental analyses of two of organo-Zn-stevensites. The Zn / Si ratio is 0.70–0.75 for stevensite, where the amount of Zn^{2+} is a sum of Zn^{2+} in the interlayer space and the layer. With organo-Zn-stevensite the Zn / Si ratio decreased due to the absence of Zn^{2+} in the interlayer space. The C / N ratio is around 19 (theoretically 20). All Si initially present was recovered in the product, but around 20% of Zn^{2+} had not been precipitated (the molar Zn / Si ratio was set at 0.75 in the initial reaction mixture). However, this amount of unreacted Zn^{2+} (denoted ΔZn^{2+}) can be correlated to the amount of $C_{18}C_2N$ now present for charge compensation. The absence of interlayer Zn^{2+} ions requires two alkylammonium ions for charge compensation; in that case an N^+ / ΔZn^{2+} ratio of two is expected. This is indeed the case. Moreover, "recalculating" the Zn / Si ratio, assuming the stevensite structure, resulted in values close to the theoretical stevensite value of 0.75. Thus, we synthesized a pure phase of organo-Zn-stevensite and the Zn / Si ratio reflects the true layer composition. The presence of vacancies accounts for the Zn / Si values lower than 0.75. The amount of $C_{18}C_2N$ also influences the Zn / Si ratio, which can be explained in several ways (1) the more alkyl ions are present, the more vacancies are created or (2) the used amount of $C_{18}C_2N$ is insufficient to account for all the vacancies and therefore Zn^{2+} ions are also present in the interlayer space. The latter explanation is excluded by both XRD (no additional reflection present at around 13–15 Å) and TEM results (no local areas with decreased interlayer distances, see below), only if layers with Zn^{2+} ions present in the interlayer space are not randomly distributed through the stacked platelets. Ijdo and Pinnavaia (1999) showed that the synthesis of hybrid structures, in our case both Zn^{2+} ions and $C_{18}C_2N$ as interlayer ions, is only possible in a very limited synthesis window. Finally, the calculated cation exchange capacity (CEC) is around 30–50 meq/100 g, which is considerably lower than values for montmorillonite (typically 80–120 meq/100 g clay). A lower CEC and the use of (protonated) $C_{18}C_2N$ instead of the commonly used ditallow dimethyl ammonium ions could be favorable, since the aliphatic chains could gain more conformational freedom (increase of entropy) when the layer separation increases during processing (Vaia and Giannelis, 1997b). CEC values were calculated, since CEC analysis methods known to the authors require cation exchange in aqueous dispersions, which is not possible in the case of hydrophobic organoclays.

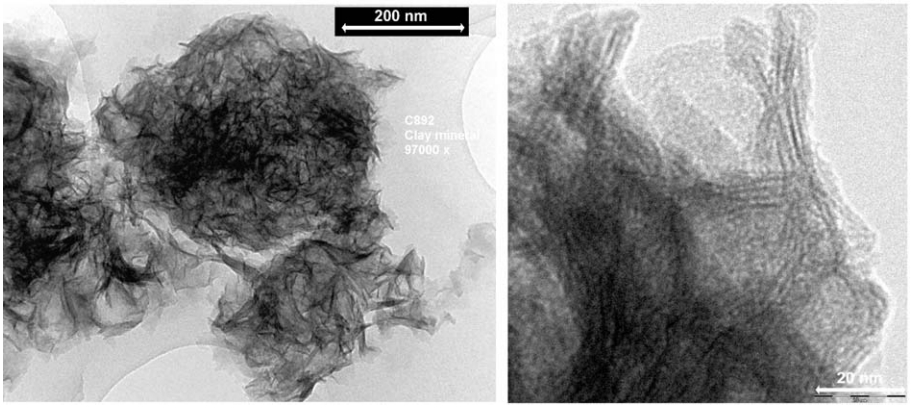

Fig. 3. TEM images of organo-Zn-stevensite powder at different magnifications.

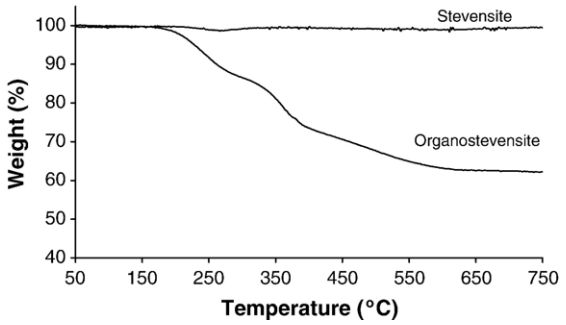

Fig. 4. TGA results of Zn-stevensite and organo-Zn-stevensite.

TEM images (Fig. 3) show agglomerates with a plate-like morphology displaying an increased interlayer spacing. Lateral size varies between 40 and 100 nm and the stacking number is low. The layer-to-layer distances are around 14–20 Å, notably larger than 4 Å (distance corresponding with the 001 reflection of Zn-stevensite having Zn^{2+} as charge-compensating cation). The material seems quite uniform and crystalline. Broadening of the (001) reflection of organo-Zn-stevensite in XRD is probably caused by a lack of thick particles. The low stacking number combined with the low CEC (Table 1) yield a better dispersion of these clay mineral platelets in polymers, despite the lower aspect ratio as compared to hectorite (Yano et al., 1997).

A 38% weight loss is observed when heating up to 800 °C (Fig. 4), which can be ascribed to the decomposing interlayer alkylammonium ions. The first weight loss step and the corresponding heat release between 200–280 °C are attributed to weakly bound alkylammonium ions, possibly adsorbed at the external basal surfaces of the particles (Le Pluart et al., 2002). In contrast, the Zn-stevensite material did not show a weight loss. This is to a large extent comparable to the results of Carrado and Xu (1998), where TGA analysis

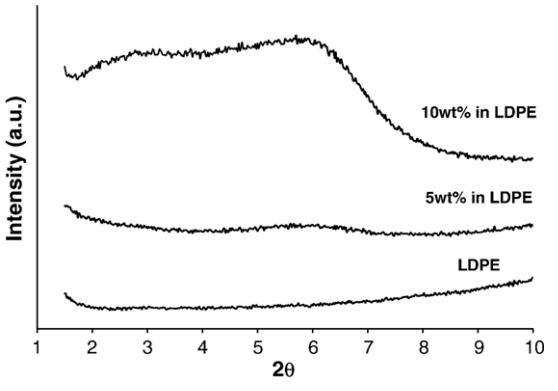

Fig. 5. XRD results of pure and organo-Zn-stevensite loaded LDPE.

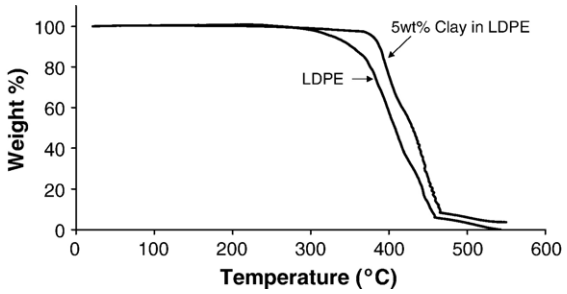

Fig. 6. TGA results of pure LDPE and 5 wt.% organo-Zn-stevensite.

of synthetic lithium hectorite resulted in a weight loss of 2.3 wt.% between 200 and 600 °C due to dehydroxylation of structural hydroxyl groups. The absence of even a small weight loss was rather unexpected, since the synthesized Zn-stevensite contains around 1 wt.% of these hydroxyl groups.

3.2. Characterization of LDPE nanocomposites

To get a first idea of the possibilities of this new material, nanocomposites of LDPE containing several concentrations of organoclay were prepared using a twin-screw extruder. Wang et al. (2001) prepared and characterized several maleated as well as non-maleated PE/clay nanocomposites. They reported that melt-blended, maleated PE with low MA levels (and also in absence of MA) and 5 wt.% of organoclay resulted in a considerable exfoliation of the clay mineral platelets. It was also stated that clay–PE nanocomposites could be obtained by proper modification of the clay mineral without the use of MA–PE. In view of these results we used pure and non-maleated PE to circumvent the occurrence of a plasticizing effect of MA on PE (Vaia and Giannelis, 1997a; Ajayan et al., 2003). Fig. 5 shows the small angle XRD of LDPE-clay hybrids at several clay loadings. At 10 wt.% (and higher, data not shown) XRD reflections appear in the small angle area, which can be

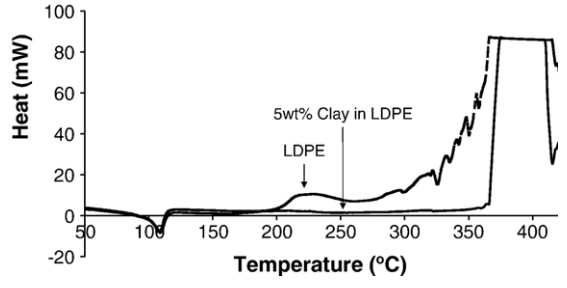

Fig. 7. DSC results of LDPE and 5 wt.% organo-Zn-stevensite in LDPE.

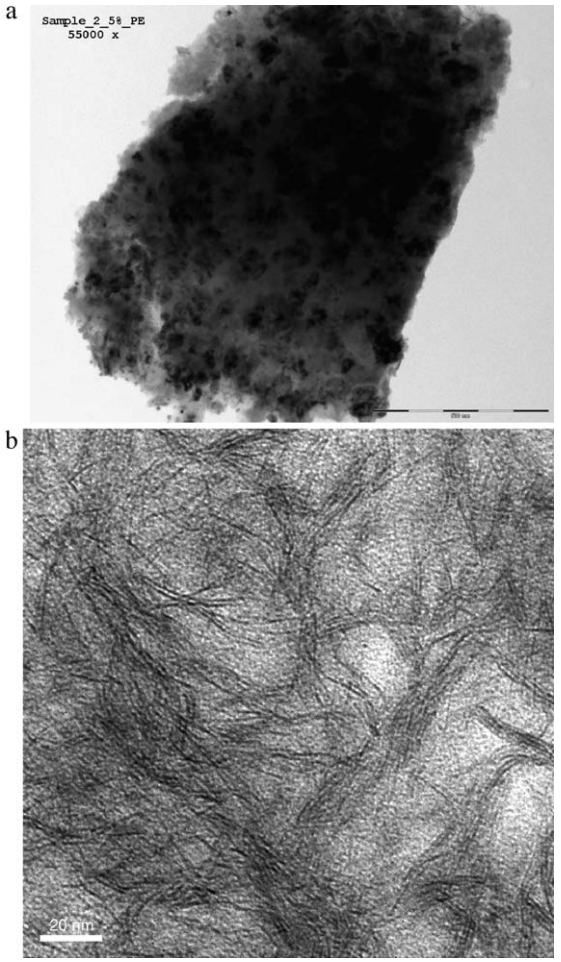

Fig. 8. TEM images of 5 wt.% organo-Zn-stevensite in (a) PE at lower magnification (scalebar 500 nm) and (b) at high magnification (scalebar 20 nm).

ascribed to organo-Zn-stevensite. Apparently, exfoliation is not or only partially achieved. When 5 wt.% of organo-Zn-stevensite is used, only a very broad and weak signal at $2\Theta = 6°$ is detected. Clearly, the dispersion of the organoclay in the polymer is much better.

Both the 5 and the 10 wt.% nanocomposite samples were subjected to ICP analysis. The Zn / Si ratios were, within the analysis error, equal to the original ratio of the organoclay powder. TGA results (Fig. 6) show that the thermal stability of LDPE significantly increases upon incorporation of 5 wt.% organo-Zn-stevensite, notably by 50 °C, up to 350 °C. Similar observations were made by Zanetti et al. (2001) for (MA-modified) PP nanocomposites and Kodgire et al. (2001). They attributed the stabilizing effect to the adsorption of volatile polymer degradation products on the silicate layers, an increased diffusion pathway and a decreased permeability of oxygen in the polymer caused by the dispersed clay mineral platelets inside the polymer material. The enhanced stability of the organoclay–PE nanocomposites is corroborated by the results of DSC measurements (Fig. 7). Apart from the evaporation of a small amount of water below 110 °C, no thermal degradation is observed below 360 °C for the 5 wt.% organoclay–PE nanocomposite. Pure LDPE starts to decompose already at 200 °C.

The use of TEM in combination with XRD for the identification of an exfoliated nanocomposite is strongly recommended, since at loadings of 5 wt.% and lower, XRD has its limitations (Morgan and Gilman, 2003). At lower magnification (Fig. 8a), small clay mineral particles were present in the PE, indicating that not all the organo-Zn-stevensite particles have been completely exfoliated. Nevertheless, the clay mineral dispersion can be considered sufficient since the clay mineral related reflections were absent in the XRD diagram of 5% clay mineral (Fig. 5). At higher magnification (Fig. 8b), delamination of the mineral particles was observed. This indicates that the organo-Zn-stevensite material exfoliated in LDPE, without the use of MA.

4. Conclusions

Organo-Zn-stevensite with intercalated dimethyl octadecylammonium cations was synthesized. The clay mineral is of high crystallinity with a low stacking number, which facilitates exfoliation in polymers like PP and PE. First results in LDPE nanocomposites, without the use of MA, point to an increased thermal stability. The Organo-Zn-stevensite is capable of exfoliation (observed with XRD and TEM) and improves properties of polymers without the use of MA.

Acknowledgements

The authors wish to acknowledge the members of the analytical service group of Engelhard De Meern B.V. for their technical assistance. Prof. John Geus is thanked for performing the TEM images. Kees Bayense and Annemarie Beers of Engelhard and Dennis Lensveld are gratefully acknowledged for their contributions during discussions and for revision of the manuscript. Marten Ubbink of Holland Colours N.V. is thanked for the nanocomposite preparation.

References

Ajayan, P.M., Schader, L.S., Braun, P.V., 2003. Nanocomposite Science and Technology. Wiley-VCH Verlag, Weinheim.

Alexandre, M., Dubois, P., 2000. Polymer-layered silicate nanocomposites: preparation, properties and uses of a new class of materials. Mater. Sci. Eng. 28, 1–63.

Bauer, P.M., Hanlon, D.J., Menking, W.R., 1993. Process for producing bentonite clays exhibiting enhanced solution viscosity properties. US Patent 5,248,641.

Beall, G.W., 2003. The use of organo-clays in water treatment. Appl. Clay Sci. 24, 11–20.

Carrado, K.A., 2000. Synthetic organo- and polymer-clays: preparation, characterization, and materials applications. Appl. Clay Sci. 17, 1–23.

Carrado, K.A., Xu, L., 1998. In situ synthesis of polymer–clay nanocomposites from silicate gels. Chem. Mater. 10, 1440–1445.

Carrado, K.A., Thiyagarajan, P., Song, K., 1997. A Study of organohectorite clay crystallization. Clay Miner. 32, 29–40.

Cody, C.A., Kemnetz, S.J., 1997. Process for the removal of heavy metals from aqueous systems using organoclays. US Patent 5,667,694.

Giannelis, E.P., 1996. Polymer layered silicate nanocomposites. Adv. Chem. 8, 29–35.

Gilman, J.W., Jackson, C.L., Morgan, A.B., Harris, R., Manias, E., Giannelis, E.P., Wuthenow, M., Hilton, D., Philips, S.H., 2000. Flammability properties of polymer-layered-silicate nanocomposites. Polypropylene and polystyrene nanocomposites. Chem. Mater. 12, 1866–1873.

Ijdo, W.L., Pinnavaia, T.J., 1999. Solid solution formation in amphiphilic organic–inorganic heterostructures. Chem. Mater. 11, 3227–3231.

Kausch, C., Verrocchi, A., Pomeroy III, J.E., Peterson, K.M., Payne, P.F., 2002. Flame resistant polyolefin compositions containing organically modified clay. US Patent 6,414,070.

Kawasumi, M., Hasegawa, N., Kato, M., Usuki, A., Okada, A., 1997. Preparation and mechanical properties of polypropylene–clay hybrids. Macromolecules 30, 6333–6338.

Kloprogge, J.T., Komarneni, S., Amonette, J.E., 1999. Synthesis of smectite clay minerals: a critical review. Clays Clay Miner. 47, 529.

Kloprogge, J.T., Hammond, M., Hickey, L., Frost, R.L., 2001. A new low temperature synthesis route of fraipontite $(Zn,Al)_3(Si,Al)_2O_5(OH)_4$. Mater. Res. Bull. 36, 1091–1098.

Knudson Jr, Milburn I., Jones T.R., 1987. Process for manufacturing organoclays having enhanced gelling properties. US Patent 4,664,842.

Kodgire, P., Kalgaonkar, R., Hambir, S., Bulakh, N., Jog, J.P., 2001. PP/clay nanocomposites: effect of clay treatment on morphology and dynamic mechanical properties. J. Appl. Polym. Sci. 81, 1786–1792.

Kurokawa, Y., Yasuda, H., Oya, A., 1996. Preparation of a nanocomposite of polypropylene and smectite. J. Mater. Sci. Lett. 15, 1481–1483.

Le Pluart, L., Duchet, J., Sauterau, H., 2002. Surface modifications of montmorillonite for tailored interfaces in nanocomposites. J. Adhes. 78, 645–662.

Maiti, P., Yamada, K., Okamoto, M., Ueda, K., Okamoto, K., 2002. New polylactide/layered silicate nanocomposites: role of organoclays. Chem. Mater. 14, 4654–4661.

Manias, E., Touny, A., Wu, L., Strawhecker, K., Lu, B., Chung, T.C., 2001. Polypropylene/montmorillonite nanocomposites. Review of the synthetic routes and materials properties. Chem. Mater. 13, 3516–3523.

Mehta, S.D., Shankernarayanan, M.J, Mavridis, H., 2003. Propylene polymer composites having improved melt strength. US Patent 6,583,209.

Morgan, A.B., Gilman, J.W., 2003. Characterization of polymer-layered (clay) nanocomposites by transmission electron microscopy and x-ray diffraction: a comparative study. J. Appl. Polym. Sci. 87, 1329–1338.

Ogawa, M., Kuroda, K., 1997. Preparation of inorganic–organic nanocomposites through intercalation of organoammonium ions into layered silicates. Bull. Chem. Soc. Jpn. 70, 2593–2618.

Orlemann, J.K., 1972. Process for producing hectorite-like clays. U.S. Patent 3,666,407.

Pozsgay, A., Papp, L., Frater, T., Pukanszky, B., 2001. Polypropylene/montmorillonite nanocomposites prepared by the delamination of the filler. Prog. Colloid & Polym. Sci. 117, 120–125.

Prihod'ko, R., Sychev, M., Hensen, E.J.M., Van Veen, J.A.R., Van Santen, R.A., 2002. Preparation, characterization and catalytic activity of non-hydrothermally synthesized saponite-like materials. Stud. Surf. Sci. Catal. 142, 271–278.

Reichert, P., Nitz, H., Klinke, S., Brandsch, R., Thomann, R., Mulhaupt, R., 2000. Poly(proylene)/organoclay nanocomposite formation: influence of compatibilizer functionality and organoclay modification. Macromol. Mater. Eng. 275, 8–17.

Reinholdt, M., Miehe-Brendle, J., Delmotte, L., Tuilier, M.-H., Le Dred, R., Cortes, R., Flank, A.-M., 2001. Fluorine route synthesis of montmorillonites containing Mg or Zn and characterization by XRD, thermal analysis, MAS NMR, and EXAFS spectroscopy. Eur. J. Inorg. Chem. 11, 2831–2841.

Tateyama, H., Tsunematsu, K., Kimura, K., Hirosue, H., Jinnai, K., Furusawa, T., 1993. Method for producing fluorine mica US Patent 5,204,078.

Usui, K., Sato, T., Tanaka, M., Mizoguchi, Y., Takahashi N., 1986. Synthetic fraipontite and process for preparation thereof. US Patent 4,626,420.

Usui, K., Sato, T., Tanaka, M., 1987. Process for preparation of synthetic crystalline zinc silicate mineral having a sauconite, willemite or hemimorphite structure. US Patent 4,681,749.

Vaia, R.A., Giannelis, E.P., 1997a. Lattice model of polymer melt intercalation in organically-modified layered silicates. Macromolecules 30, 7990–7999.

Vaia, R.A., Giannelis, E.P., 1997b. Polymer melt intercalation in organically-modified layered silicates: model predictions and experiment. Macromolecules 30, 8000–8009.

Vaia, R.A., Giannelis, E.P., 2001. Polymer nanocomposites: status and opportunities. MRS Bull. 26, 394–401.

Vogels, R.J.M.J. Non-hydrothermally synthesized trioctahedral smectites. Ph.D. Thesis, Utrecht University, The Netherlands.

Vogels, R.J.M.J., Geus, J.W., 2001. Synthetic swelling clay minerals. US Patent 6,187,710.

Vogels, R.J.M.J., Kloprogge, J.T., Geus, J.W., 2005. Synthesis and characterization of saponite clays. Am. Miner. 90, 931–944.

Wang, K.H., Choi, M.N., Koo, C.M., Choi, Y.S., Chung, I.J., 2001. Synthesis and characterization of maleated polyethylene/clay nanocomposites. Polymer 42, 9819–9826.

Yano, K., Usuki, A., Okada, A., 1997. Synthesis and properties of polyimide–clay hybrids films. J. Polym. Sci., A, Polym. Chem. 31, 2289–2294.

Zanetti, M., Camino, G., Reichert, P., Mulhaupt, R., 2001. Thermal behaviour of poly(propylene) layered silicate nanocomposites. Macromol. Rapid Commun. 22, 176–180.